

A Printed Semi-Circular Disc UWB MIMO/Diversity Antenna with Cross Shape Slot Stub

Raj Kumar¹ · Neha Pazare²

Published online: 13 July 2016
© Springer Science+Business Media New York 2016

Abstract The paper presents a combination of microstrip and CPW fed semicircular patch antennas for UWB polarization diversity applications. The overall size of the diversity antenna is 40 mm × 40 mm × 1.6 mm. Both the patches are placed in an orthogonal arrangement to provide polarization diversity and to improve the isolation. The measured impedance bandwidth is from 3.0 to 10.6 GHz for the CPW fed antenna while it is from 2.7 to 11.0 GHz for the microstrip fed antenna. An extra operating band is obtained at around 1.2 GHz (measured) due to the common ground plane. The measured isolation is between 20 and 25 dB over most of the band. A detail parametric study is done to analyze the effect of the different parameters on the return losses of both the ports and the isolation between them. The radiation patterns are measured and found to be omnidirectional in the H-plane and dumb-bell shape in the E-plane. The peak gain is between 3 and 5 dBi over most of the band while the radiation efficiency is more than 80 %. Diversity parameters such as envelope correlation coefficient and diversity gain are also calculated and found to be within acceptable limits. The antennas will be useful for diversity applications in the ultra wideband region and for GSM/GPS applications in the first operating band.

Keywords UWB antenna · Diversity antenna · Microstrip feed · CPW feed · Patch antenna

1 Introduction

In 2002, the Federal Communications Commission (FCC) has released for unlicensed use, a frequency band from 3.1 to 10.6 GHz, named the Ultra Wide Band (UWB). UWB has many advantages such as huge bandwidth, low power, carrier less transmission and high

✉ Raj Kumar
drrk1963@gmail.com

¹ AE, ARDE, Pune 411 021, India

² DIAT(DU), Girinagar, Pune 411 025, India

data rate (more than 200 Mbps) when compared to conventional narrowband communication systems. Hence, this technology has attracted many researchers to work in this field. Most of the UWB antennas proposed in the literature use the microstrip feed or the CPW feed technique. Some of the CPW fed patch antennas working over UWB are reported [1–3]. In [1], a $25 \times 25 \times 1.6 \text{ mm}^3$ CPW fed UWB patch antenna is proposed. The antenna has an inverted L-strip patch and offers good impedance matching from 2.6 to 13.04 GHz covering the entire FCC band. In [2], a novel CPW fed monopole antenna for WiMAX/WLAN applications is proposed. The antenna has an overall size of $25 \times 25 \text{ mm}^2$ and operates over three bands covering 2.14–2.85, 3.29–4.08 and 5.02–6.09 GHz. In [3], an L-shaped planar monopole and an I-shaped open stub antenna is proposed for ultra wide band applications. The antenna has a bandwidth covering the 3–11 GHz frequency range. The antenna has overall size of $25 \times 30 \text{ mm}^2$. Some of the partial microstrip fed patch antennas are reported [4, 5]. In [4], an UWB slot antenna fed by CPW is introduced having triple band notch function. The overall size of the antenna is $40 \times 22 \times 0.8 \text{ mm}^3$. The antenna has a bandwidth from 2 to 12 GHz including notches at 2.4, 3.5 and 5.5 GHz with VSWR ≤ 2 . A small UWB planar monopole antenna is proposed in [5] consisting of diamond shaped patch covering the frequency bands, 1.3, 1.8, 2.4 and 3.1–10.6 GHz. The antenna has overall size of $16 \times 22 \text{ mm}^2$.

A problem encountered in UWB high data rate wireless communication systems is the fading of the information signal. In order to reduce this fading and increase the capacity of the channel, antenna diversity technique is used, where two or more antennas are placed at the transmitter and the receiver. Some diversity antennas are published in open literature [6–10]. In [6–8], by using orthogonal orientation between the elements, wideband inter-port isolation as good as 15–17 dB is reported over the UWB spectrum. In [9], a polarization diversity antenna having overall size more than $104 \times 108 \text{ mm}^2$ is introduced, which consists of two fork shaped CPW-fed antennas placed orthogonally with an inverted U-shaped strip. The antenna is quad band having frequencies centered at 1.9, 2.4, 3.5 and 5.5 GHz. In [10], a multiband E-shaped monopole with overall size more than $70 \times 76 \text{ mm}^2$ is introduced for multiple-input–multiple-output (MIMO)/Diversity applications. The antenna covers 2.4, 5.4 and 5.8 GHz frequencies of WLAN. In [11–15], the isolation enhanced by minimising the induced current over the common ground by modifying it. Several different geometries have been reported as a defected (partially cutaway and/or extended) ground such as a tree-like structure [11], two T-shaped stubs [12], multiple stubs [13], inverted Y-slots [14] and a rectangular slot [15] to improve the inter-port isolation between the two antennas. The results published in [11–15] reveal the two-port isolation level in the range of 15–20 dB in operating band. In all, it clear either the diversity antenna reported having complex structure with large size or low isolation between two-port.

The antenna proposed in this paper consists of two orthogonally placed semi-circular metallic patches excited using microstrip and CPW feed lines with overall size of $40 \text{ mm} \times 40 \text{ mm} \times 1.6 \text{ mm}$. To reduce the coupling between the two radiating elements, a cross shape slot stub is placed at the intersection of the ground planes of the two antennas. The antennas offer impedance bandwidth satisfying the FCC UWB criteria while the isolation varies from 20 to 25 dB over most of the operating band. In the following sections, the antenna geometry is outlined followed by simulated and measured results, and parametric studies.

2 Antenna Design

Figure 1 shows detailed geometry of the proposed diversity antenna which is printed on FR-4 substrate. The substrate has relative permittivity of 4.4, loss tangent of 0.025 and thickness of 1.66 mm. The overall size of the proposed antenna is $L \times W$. The proposed antenna consists of two semi-circular shape monopoles with one CPW fed and other microstrip fed. The semi-circular shape discs have a radius $r = 10$ mm and rotated by 45° from the vertical. The ground plane consists of various slits of semicircular and rectangular shapes inserted for the purpose of impedance matching. One half of the ground plane on the CPW and the microstrip side is shaped in the form of a triangle. The triangular ground plane on the CPW side has one of its corners blended. To improve the isolation, a cross shaped slot is added in the ground plane between the two antennas. The optimized dimensions of the antenna are given in Table 1.

3 Simulation of Individual Monopole Antenna and Diversity Antenna

The two port antenna consists of two monopoles; one fed by a CPW and one fed by a microstrip feed. The monopoles have a semi-circular disc shape. The return loss characteristics of the individual monopoles (without the other element) are compared with the return loss characteristic of the combined structure in Fig. 2a, b. The impedance bandwidths are also compared. Here, the impedance bandwidth is defined as the range of frequencies over which the reflection coefficient is below -10 dB. A reflection coefficient < -10 dB implies a mismatch (between the antenna element and the 50Ω connected port) of $< 10\%$ or more than 90% of the input energy accepted by the antenna. A 6-dB return loss is also used for marking the bandwidth in some applications such as mobile phones. It is seen that while the impedance bandwidth of the microstrip fed monopole is from 2.3 to 11 GHz, the impedance bandwidth of the single CPW fed monopole is from 2.1 to

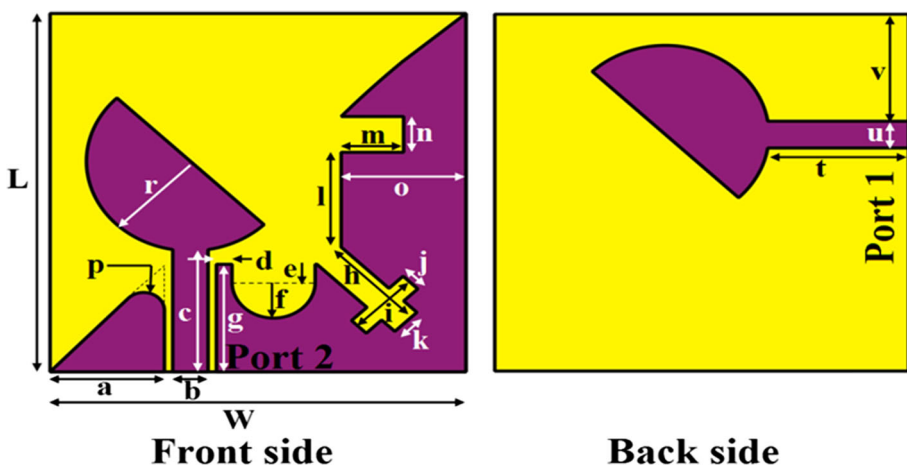


Fig. 1 Geometry of the proposed antenna

Table 1 Optimized dimensions of the antenna (in mm)

Label	Size	Label	Size	Label	Size	Label	Size
a	11	E	2	i	7	m	6
b	3.4	F	4	j	2	n	4
c	13.7	G	12	k	3	o	12
d	1.5	H	11.5	l	10.6	p	2
r	10	T	13.5	u	3	v	12
L	40	W	40				

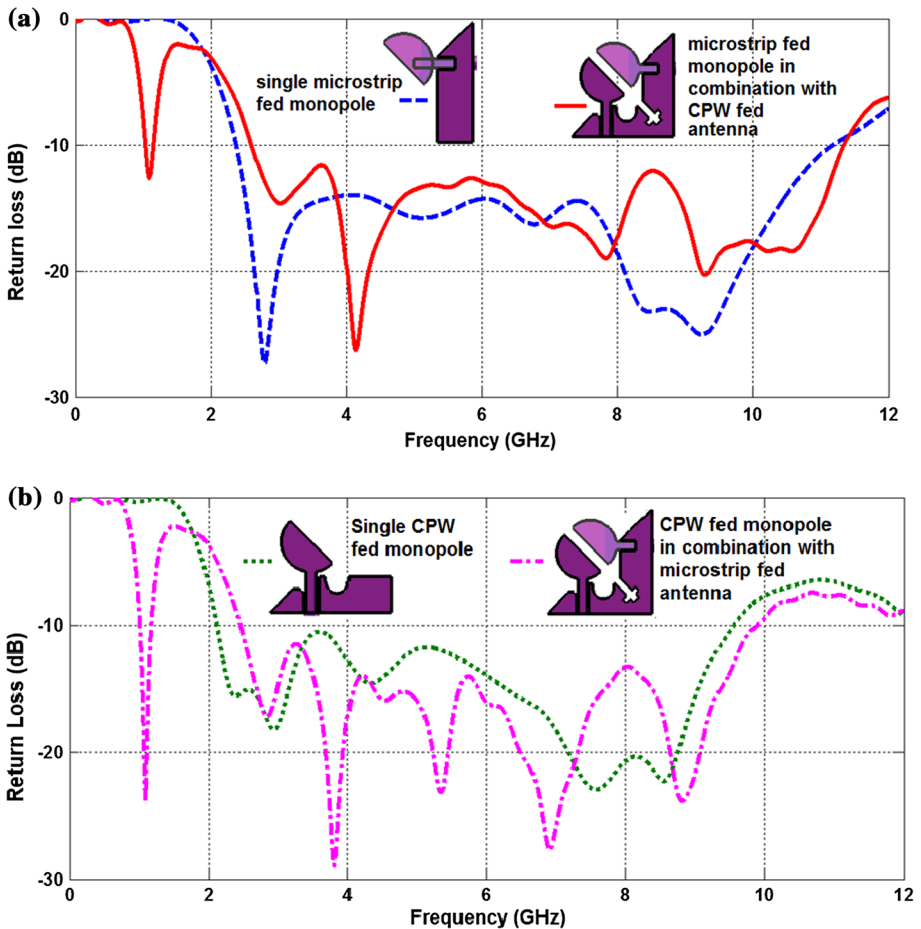


Fig. 2 Comparison of the return loss of **a** the microstrip fed without and with the CPW fed element and **b** the CPW fed antenna without and with the microstrip element

9.6 GHz. When the antennas are combined and a cross shaped slot is added to the ground plane, the impedance bands on both the sides are shifted to the higher side along with some extra resonances (dips seen in the reflection coefficient curves) in the operating band. More importantly, an extra resonance is obtained near 1 GHz due to the extended ground plane.

4 Simulated and Measured Results

The proposed antenna is simulated on CST Microwave Studio and fabricated with the optimized dimensions. The fabricated prototype of the proposed antenna is shown in Fig. 3a. A Vector Network Analyzer (Rohde and Schwarz ZVA-40) is used to measure the return loss and the isolation of the fabricated diversity antenna. The simulated and measured S-parameters are compared and shown in Fig. 3b–d. The return loss is taken as the negative of the reflection coefficient S_{11} and isolation is taken as the negative of the transmission parameter S_{21} . In general, a good agreement between the simulated and measured results can be seen while some frequency shift between the two (for all the curves) is due to the reflection from the SMA connector and uncertainty in dielectric substrate and fabrication tolerances.

From the return loss curve of the CPW fed antenna (Port 1), it is seen that the measured bandwidth starts from 3 GHz and extends up to 10.6 GHz, whereas in case of the microstrip fed antenna (Port 2), the bandwidth is from 2.7 to 11 GHz. An additional resonance near 1.1 GHz for the simulated curve and near 1.2 GHz for the measured curve is also seen. This band is obtained due to the extended ground plane in case of a two port antenna and does not appear in case of individual monopole (Fig. 2). Figure 3d shows the isolation between both the radiators. It is more than 20 dB at higher frequencies from 5.3 GHz onwards and around 15 dB at lower frequencies.

5 Current Distribution

Figure 4 shows the simulated surface current distribution of the proposed antenna at various frequencies. Figure 4a shows the current distribution at 3, 4.14, 5.53 and 7.85 GHz when the CPW fed antenna (Port 1) is excited and Fig. 4b shows the current distribution at 2.85, 3.82, 5.35 and 6.09 GHz when the microstrip fed antenna (Port 2) is excited. The frequencies at which the current distribution is shown are the resonance frequencies seen in the return loss curves of the CPW fed antenna (S_{11}) and the microstrip fed antenna (S_{22}). It

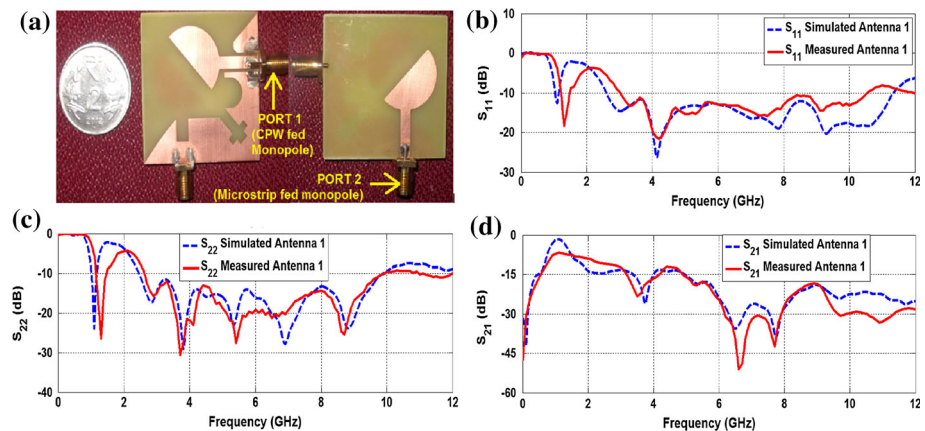


Fig. 3 a Fabricated antenna, b S_{11} , return loss of the CPW fed antenna, c S_{22} , return loss of the microstrip fed antenna, d S_{21} , coupling between the ports

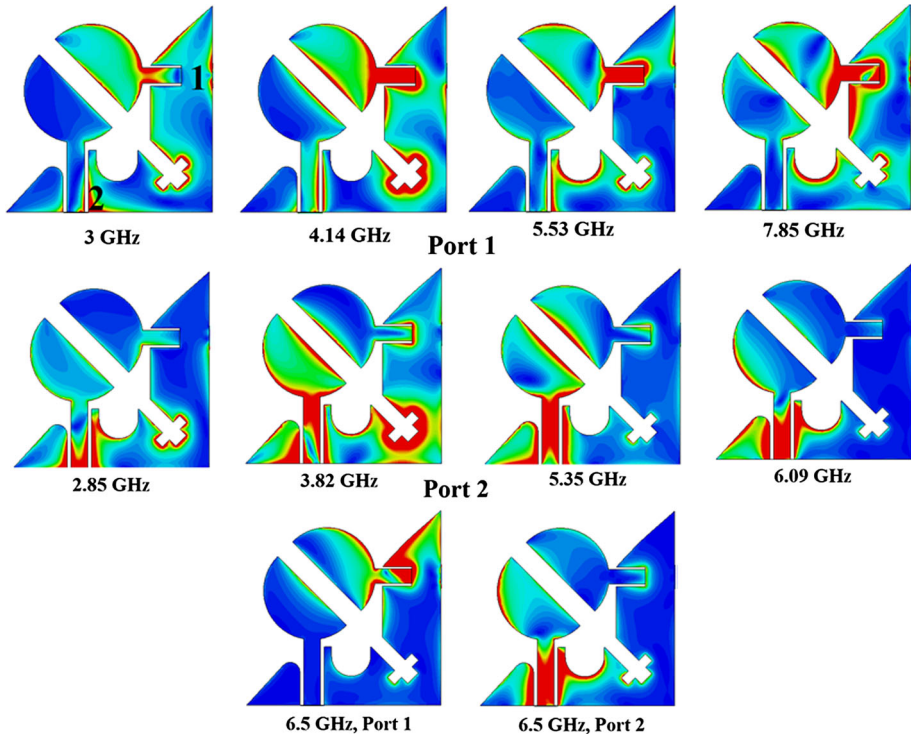


Fig. 4 Surface current distribution for the CPW fed antenna (Port 1 excitation) and the microstrip fed antenna (Port 2 Excitation) at some frequencies

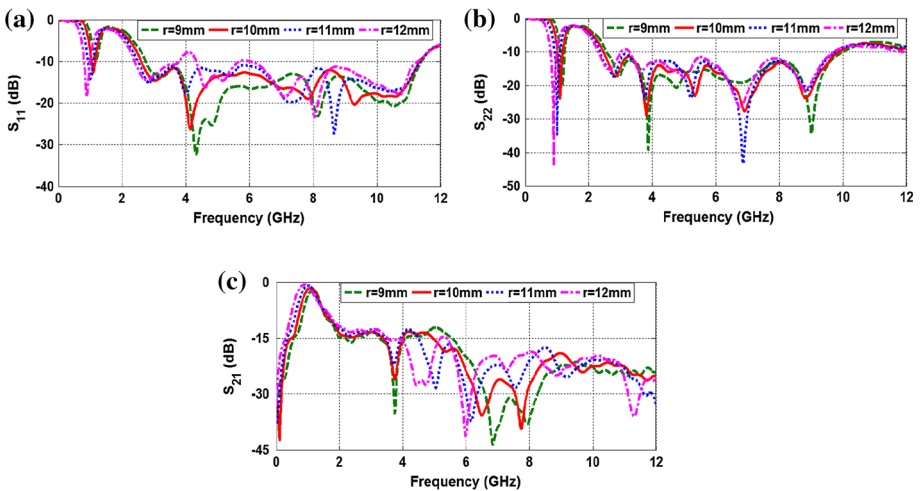


Fig. 5 Simulated results of **a** CPW fed antenna return loss, S_{11} **b** microstrip fed antenna return loss, S_{22} and **(c)** Coupling, S_{21} for different values of 'r'

is seen that among all the frequencies, the current distribution is more on the semi-circular patch at 4.14 GHz in case of the CPW fed antenna (Port 1 excitation) and at 3.82 GHz in case of the microstrip fed antenna (Port 2 excitation). Hence, it can be said that these resonances are directly related to the patch for those two ports. Also shown in the bottom layer of Fig. 4 are the current distributions at one of the frequencies where the isolation is good (6.5 GHz) as seen from the S_{21} curve. From the figure, it can be seen that the cross shape slot stub placed in the ground plane absorbs some of the current and helps in improving the isolation by blocking the flow of current into the other port.

6 Parametric Studies

A detailed study of the effects of the various parameters on the performance of the antenna was carried out and explained in the following section. The parametric study is done to analyze how the various parameters affect the results and to obtain the optimized values.

6.1 Radius of the Patch

Figure 5 shows different curves of the simulated S-parameters for various values of radius of the semi-circular patch given by 'r'. As seen from Fig. 5a, b, as the radius increases, the lower cutoff frequency and the resonance near 3 GHz shift to the lower side. The first resonance near 1 GHz is also found to be lowered. When the radius is increased beyond 10 mm, the return loss degrades at 4, 6 and 8 GHz for the CPW fed antenna (Port 1) and at 3.2 and 5.8 GHz for the microstrip fed antenna (Port 2). On the other hand, a smaller value of radius such as 9 mm has decreased the isolation at 5 GHz. Hence, the radius of patch is fixed to 10 mm.

6.2 Depth of the Slot Over the Microstrip Line

Figure 6 shows the variations in the S-parameters depending upon the depth of the slot placed over the microstrip line and indicated by 'm' in Fig. 1. For $m = 5$ mm, the return loss (negative of S_{11}) is more over most of the frequency band at 3.7 GHz. By increasing the value of 'm', the upper cut-off frequency (beyond which S_{11} increases above -10 dB) reduces and hence the bandwidth is reduced but the return loss improves (increases) near 3.7 GHz. Hence, the depth of the slot was fixed at 6 mm. The isolation did not get much affected due to the variations in value of 'm' as shown in Fig. 6b.

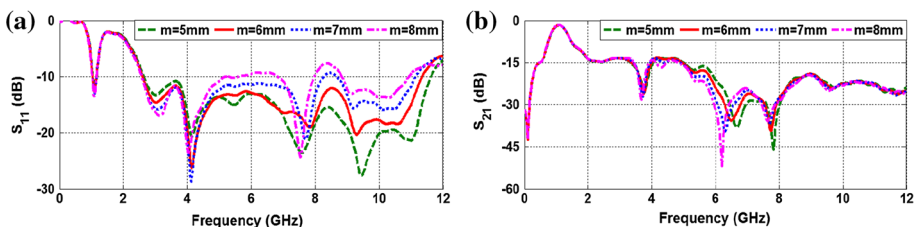


Fig. 6 Simulated results of **a** CPW fed antenna return loss, S_{11} and **b** coupling, S_{21} for different values of 'm'

6.3 CPW Ground Corner Blend Value

The blending (rounding) of the upper left edge of the CPW ground plane has its effect on the return loss of the CPW fed monopole as seen from Fig. 7. The radius of the blending arc is denoted by 'p' in Fig. 1. For $p = 1$ mm, return loss is <10 dB over the frequency range of 7–8.3 GHz. Hence, instead of a continuous operating band ($S_{11} < -10$ dB) from 3 to 10 GHz, two separate bands are obtained. When the blend radius is increased, return loss increases near 8 GHz and an ultra wide impedance bandwidth from 2.3 to 10 GHz is obtained. Hence the value of the blend was fixed at $p = 2$ mm.

6.4 Radius of Semicircular Slit in the Ground Plane

The effect of the radius of the semi circular slit in the ground plane on the return loss and the isolation is shown in Fig. 8. This radius is denoted by 'f' in Fig. 1. It can be seen from Fig. 8a that the variation in the radius of the semicircle has not much affected the return loss of the CPW fed monopole antenna. But from Fig. 8b, it is seen that the isolation in the frequency range of 6–9 GHz significantly depends on this radius. For $f = 2$ mm, the isolation is around 15 dB in the region and a gradual increase in the radius has improved the isolation. At the same time, an increase in the radius to beyond 4 mm deteriorates the return loss near 3 GHz and hence not followed.

6.5 Gap Between Microstrip Fed Patch and Ground

The next parameter analyzed is the height of the microstrip fed semi-circular patch above the ground plane. This parameter is denoted by 'x' in the study and in terms of the antenna parameters shown in Fig. 1 and valued in Table 1, is equal to 't - o'. The design was analyzed for different values of x and the effects on the return loss and the isolation are shown in Fig. 9. The separation between the patch and the ground is very crucial for the return loss of the antenna as it directly controls the amount of coupling between the antenna and the ground plane. As shown in Fig. 9a, a lower value of the separation deteriorates the return loss characteristic (decreases its magnitude) of the microstrip fed monopole over most of the frequencies whereas a higher value such as 3.5 mm deteriorates (decreases) it near 8 GHz. Hence, the gap is optimized to 1.5 mm. The gap also effects the isolation particularly at higher frequencies. While a smaller gap improves the isolation on

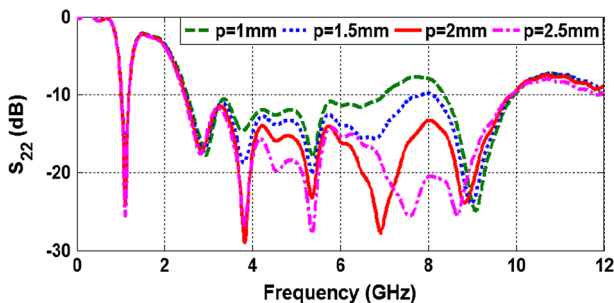


Fig. 7 Simulated values of microstrip fed antenna return loss, S_{22} for different values of 'p'

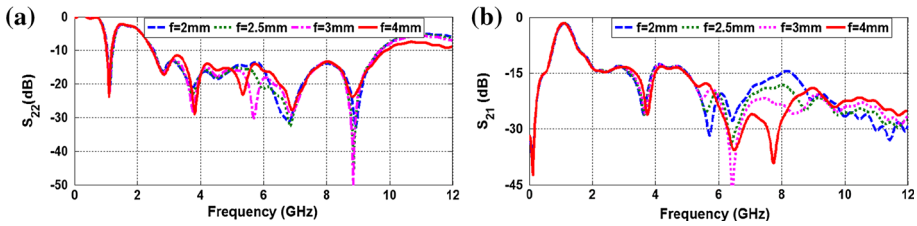


Fig. 8 Simulated values of **a** microstrip fed antenna return loss, S_{22} and **b** coupling, S_{21} for different values of ‘f’

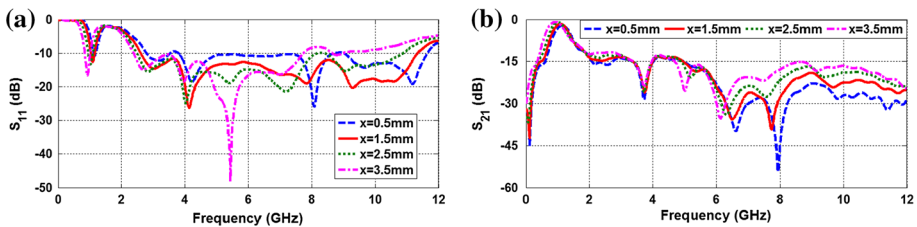


Fig. 9 Simulated values **a** CPW fed antenna return loss, S_{11} and **b** coupling, S_{21} for different values of ‘x’

higher frequencies, it deteriorates the return loss; increasing the gap deteriorates the isolation. Hence, an intermediate value of $x = 1.5$ mm was chosen for fabrication.

7 Radiation Patterns, Efficiency and Peak Gain

7.1 Radiation Patterns

The farfield radiation of the proposed antenna consisting of the simulated and measured E-plane and H-plane radiation patterns are shown in Fig. 10 for both the ports. When the CPW fed antenna (Port 1) is excited, the microstrip feed (Port 2) is terminated by a 50-ohm line and vice versa. The radiation patterns are measured in an in-house anechoic chamber and the measured results compared with the simulated ones show a proper agreement. The co-polarized gain is seen to have a dumbbell shape in the E-plane whereas an omnidirectional patterns in the H-plane. The radiation patterns are stable over the operating range of the antenna. The radiation patterns for the CPW fed antenna (Port 1) are shown at 4.0, 5.6, 7.4 and 10.0 GHz for the E-plane and at 4.0, 5.6, 7.8 and 10.0 GHz for the H-plane. For the microstrip fed antenna (Port 2), the radiation patterns are shown at 4.0, 5.6, 7.4 and 10 GHz for the E-plane and at 4.0, 6.0, 7.4 and 10.0 GHz for the H-plane.

7.2 Radiation Efficiency

Next shown are the simulated radiation efficiencies at both the ports in Fig. 11. The radiation efficiency generally shows the relation between the power delivered to the antenna and the power radiated by the antenna. From the figure, it is seen that the radiation efficiency is almost above 90 % at lower frequencies and decreases gradually to 80 % at

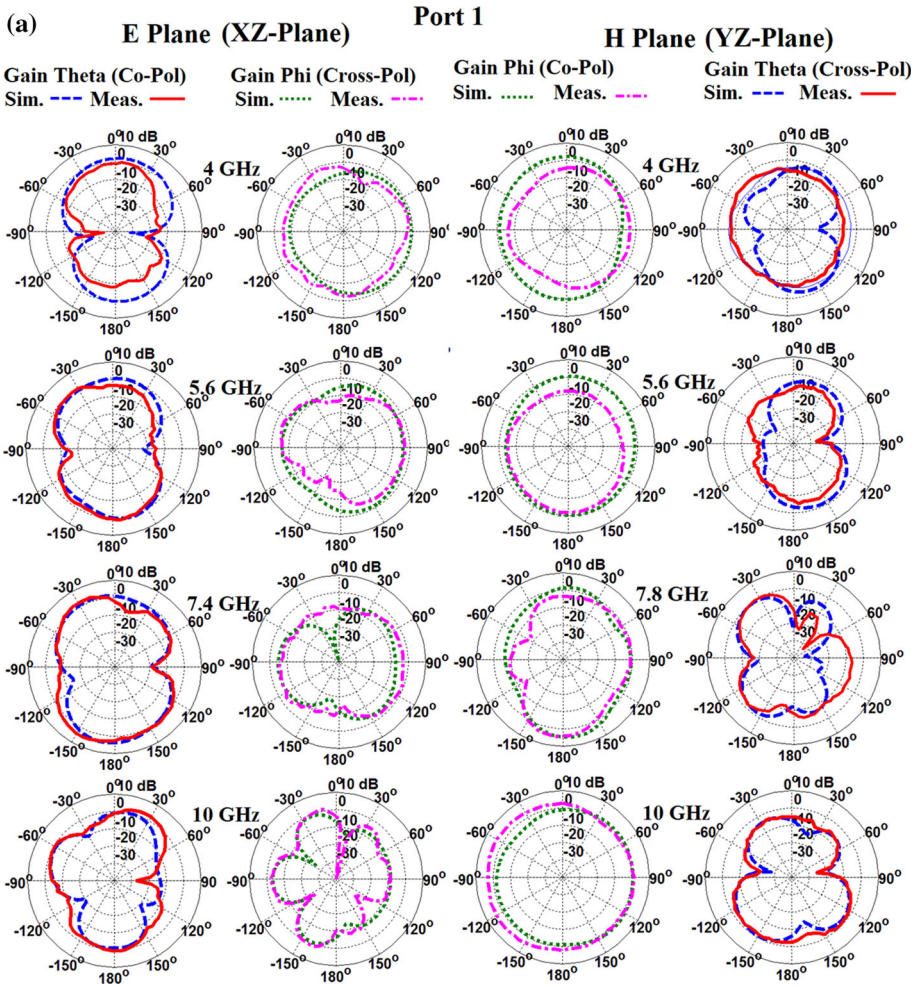


Fig. 10 Radiation patterns for the a CPW fed antenna (Port 1) and b microstrip fed antenna (Port 2)

higher frequencies. The decrease in the radiation efficiency at higher frequencies is due to the increased frequency dependent copper and substrate losses.

7.3 Peak Gain

The peak gain is simulated and measured for both the ports. The simulated and measured peak gains are compared and shown in Fig. 12. The simulated peak gains for both the ports are almost equal. In case of the measured peak gains, some difference is noted over the frequency range of 5–8 GHz. The peak gain varies between 0 and 5 dB over the operating bandwidth. The difference seen between the simulated and measured gains at lower frequencies is due to the characteristics of the reference horn antenna used in the measurement system. In general, the gains tend to increase with frequency due to an increase in the effective area of radiation at higher frequencies.

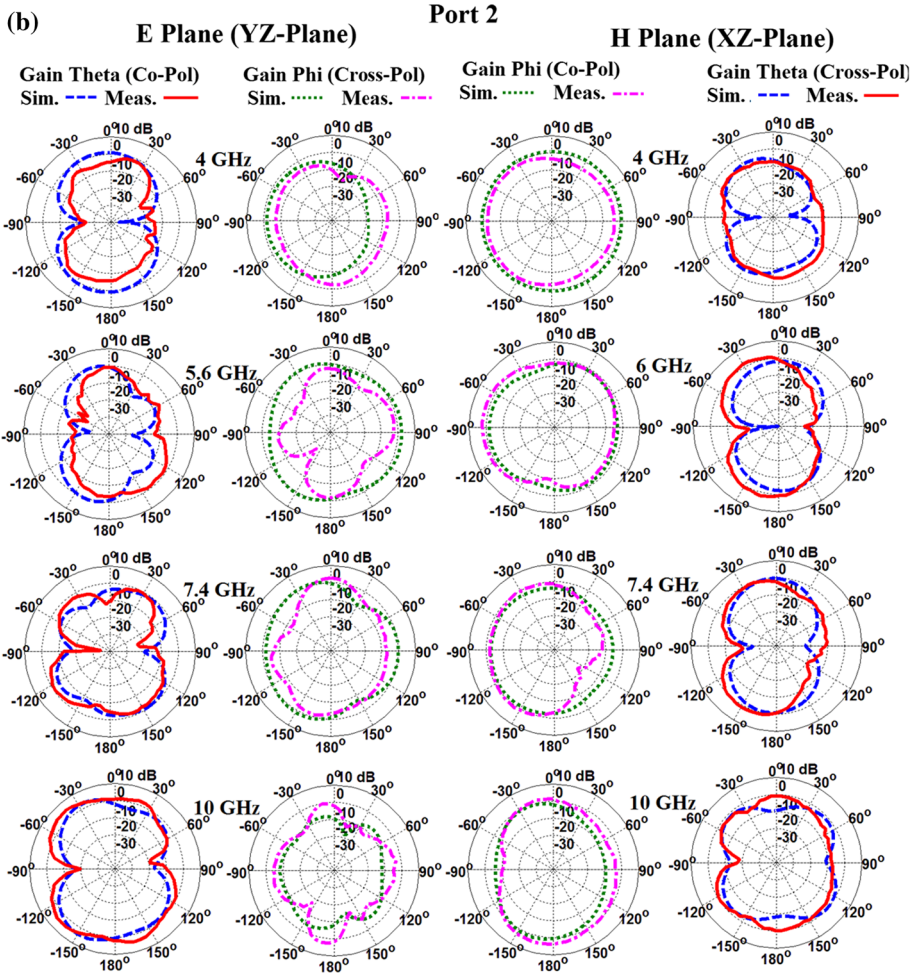


Fig. 10 continued

Fig. 11 Simulated radiation efficiencies at both the ports

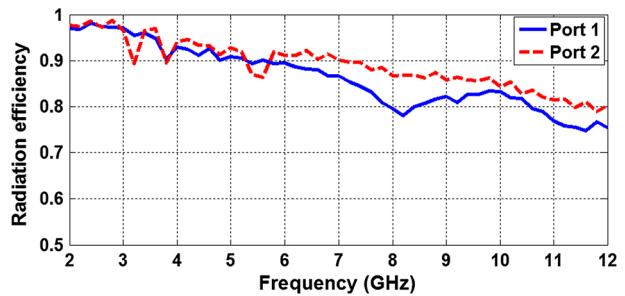


Fig. 12 Measured and simulated peak gain

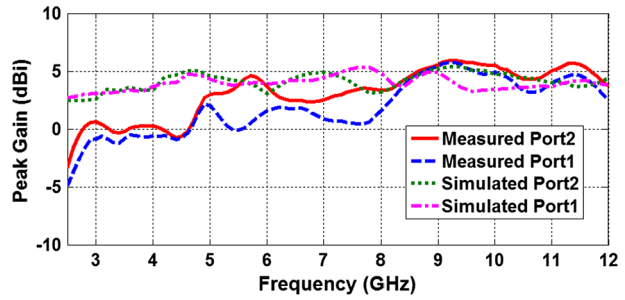
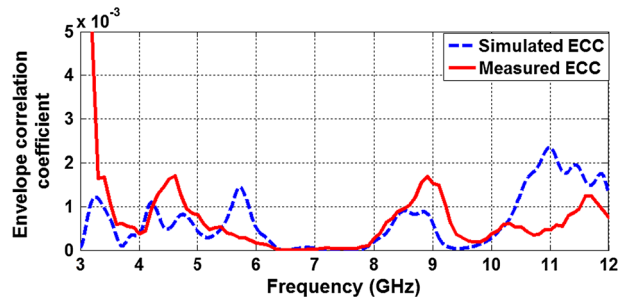


Fig. 13 Measured and simulated envelope correlation coefficient

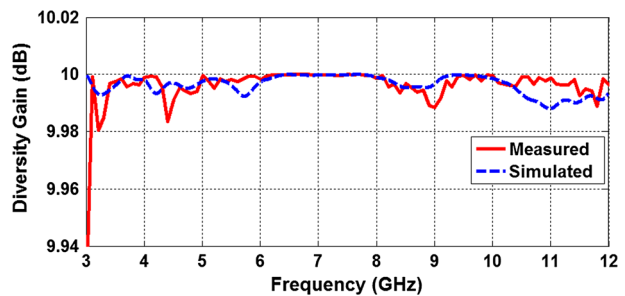


8 Diversity Parameters

8.1 Envelope Correlation Coefficient

Envelope correlation coefficient is one of the parameters used to evaluate the diversity performance of an antenna. In case of multiple antenna systems, signals from one antenna may have a correlation with the signals from the other antenna. For good diversity performance its value should be <0.5 [16, 17]. The extent to which these signals are correlated is described by the envelope correlation coefficient. The envelope correlation coefficient can be calculated from the simulated or measured Scattering parameters by using Eq. (1). This is very simple method of calculating the envelope correlation coefficient depicted in Fig. 13.

Fig. 14 Measured and simulated diversity gain



$$\rho = \frac{|S_{11}^* S_{21} + S_{12}^* S_{22}|^2}{\left| \left(1 - |S_{11}|^2 - |S_{21}|^2\right) \left(1 - |S_{22}|^2 - |S_{12}|^2\right) \right|} \quad (1)$$

It can be seen from the figure, that the simulated and measured correlation coefficients are below 0.002 and hence very less as desired.

8.2 Diversity Gain

Diversity gain is another important parameter for evaluating the diversity performance of the proposed antenna. Usually, it is evaluated when the envelope correlation coefficient < 0.5 [17]. Its value should be closer to 10. Equation (2) is used to calculate the diversity gain of the antenna [18]. Equation (2) implies that the diversity gain is related to the envelope correlation coefficient and a lower value of ECC implies a higher diversity gain. Figure 14 shows a comparison of simulated and measured diversity gain of the antenna which is almost equal to 10.

$$G = 10\sqrt{1 - |\rho_e|^2} \quad (2)$$

9 Conclusions

A semicircular patch antenna with CPW and microstrip feed is proposed for diversity applications. The patch fed by the CPW and the patch fed by the microstrip feed are placed orthogonal to each other. The antenna has a measured impedance bandwidth of 3–10.6 GHz at one of the ports (CPW feed) and a bandwidth of 2.7–11 GHz at the other port (microstrip feed). The measured isolation varies between 20 and 25 dB over much of the band. An additional operating band suitable for GSM/GPS applications is realized at 1.2 GHz due to the common ground plane. The simulated and measured results are in good agreement. The radiation patterns along with peak gain and radiation efficiency are also presented. Diversity parameters such as envelope correlation coefficient and diversity gain are also calculated and acceptable. Such type of diversity antenna is suitable for portable and mobile ultra-wideband applications. An array formed of such antennas will also be useful for high gain imaging and surveillance radar applications.

References

1. Gautam, A., Yadav, S., & Kanaujia, B. (2013). A CPW-fed compact UWB microstrip antenna. *IEEE Antennas and Wireless Propagation Letters*, 12, 151–154.
2. Liu, H., Ku, C., & Yang, C. (2010). Novel CPW-fed planar monopole antenna for WiMAX/WLAN applications. *IEEE Antennas and Wireless Propagation Letters*, 9, 240–243.
3. Kim, J., & Jee, Y. (2007). Design of ultrawideband coplanar waveguide-fed LI-shape planar monopole antennas. *IEEE Antennas and Wireless Propagation Letters*, 6, 383–387.
4. Mohammadian, N., Azarmanes, M.-N., & Soltani, S. (2009). Compact ultra-wideband slot antenna fed by coplanar waveguide and microstrip line with triple-band-notched frequency function. *IET Micro-waves, Antennas & Propagation*, 4, 1811–1817.

5. Foudazi, A., Hassani, H., & Nezhad, S. (2012). Small UWB planar monopole antenna with added GPS/GSM/WLAN bands. *IEEE Antennas and Wireless Propagation Letters*, 60, 2987–2992.
6. Rajagopalan, A., Gupta, G., Konanur, S., Hughes, B., & Lazzi, G. (2007). Increasing channel capacity of an ultrawideband MIMO system using vector antennas. *IEEE Transactions on Antennas and Propagation*, 55, 2880–2887.
7. Adamiuk, G., Zwick, T., & Wiesbeck, W. (2010). Compact, dual-polarized UWB antenna, embedded in a dielectric. *IEEE Transactions on Antennas and Propagation*, 58(2), 279–286.
8. Wang, L., & Huang, B. (2012). Design of ultra-wideband MIMO antenna for breast tumor detection. *International Journal of Antennas and Propagation*, 2012, 1–7.
9. Darvish, M., & Hassani, H. R. (2012). Quad band CPW-fed monopole antenna for MIMO applications. EuCAP 2012 1569522349.
10. Nezhad, S. M. A., & Hassani, H. R. (2010). A novel triband E-shaped printed monopole antenna for MIMO application. *IEEE Antennas and Wireless Propagation Letters*, 9, 576–579.
11. Zhang, S., Ying, Z., Xiong, J., & He, S. (2009). Ultrawideband MIMO/diversity antennas with a tree-like structure to enhance wideband isolation. *IEEE Antennas and Wireless Propagation Letters*, 8, 1279–1282.
12. Lee, J., Hong, S., & Choi, J. (2010). Design of an ultra-wideband MIMO antenna for PDA applications. *Microwave and Optical Technology*, 52(10), 2165–2170.
13. Hong, S., Chung, K., Lee, J., Jung, S., et al. (2008). Design of a diversity antenna with stubs for UWB applications. *Microwave and Optical Technology Letters*, 50, 1352–1356.
14. Najam, A., Duroc, Y., & Tedjni, S. (2011). UWB-MIMO antenna with novel stub structure. *Progress in Electromagnetics Research C*, 19, 245–257.
15. Jusoh, M., Jamlos, M. F., Kamarudin, M. R., & Malek, F. (2012). A MIMO antenna design challenges for UWB applications. *Progress in Electromagnetics Research B*, 36, 357–371.
16. Zhang, S., Ying, Z., Xiong, J., & He, S. (2009). Ultrawideband MIMO/diversity antennas with a tree-like structure to enhance wideband isolation. *IEEE Antennas and Wireless Propagation Letters*, 8, 1279.
17. Najam, A., Duroc, Y., & Tedjni, S. (2011). UWB-MIMO antenna with novel stub structure. *Progress in Electromagnetics Research C*, 19, 245–257.
18. Votis, C., Tatsis, G., & Kostarakis, P. (2010). Envelope correlation parameter measurements in a MIMO antenna array configuration. *International Journal of Communications, Network and System Sciences*, 3, 350–354.



Mr. Raj Kumar was born on 14th May 1963 in Muzaffarnagar U.P., India. He has completed his M. Sc. Degree specialized in Electronics in 1987 from University of Meerut, Meerut. He has been awarded M. Tech. and Ph. D degree in Microwave in 1992 and 1997 respectively from University of Delhi South Campus, New Delhi. He worked at CEERI Pilani from 1993 to 1994 as a Research Associate. From May 1997 to June 1998, he worked as Assistant Professor in Department of Electronics and Communications Engineering, Vellore College of Engineering (Now VIT), Vellore. He worked in DLRL (DRDO), Hyderabad as Scientist from June 1998 to August 2002 and later on came in DIAT and worked in Department of Electronics Engineering, DIAT (Deemed University), Pune till September 2012. During his stay at DIAT, he established a Microwave and Millimeter Wave Antenna Laboratory and started M. Tech. (Radar and Communication) course in the Department of Electronics Engineering in 2010. Since October 2012, he is working in ARDE, Pune. He has written several technical

papers in referred International Journal and conferences. He has presented the several papers in international conference, Chaired session, delivered the invited lecture and won the best papers award. His field of interest is Microwave components and antennas like Multiband antenna, fractal antenna, UWB antenna, slot antenna, notched antenna, Electromagnetic band-gap, frequency selective surface, filters, Multiplexers, Power dividers, Couplers, Numerical Technique, Electromagnetic Analysis and Simulation, and ANN for Microwave circuit and Antennas.



Neha Pazare was born in Maharashtra, India, on 18th February 1990. She pursued B.E. in electronics and communication from Rashtrasant Tukdoji Maharaj University, Nagpur, India in 2012. Currently she is working towards M.Tech. degree (Lasers and electro optics) from Defence Institute of Advanced Technology, Pune, India. Her research interests are in electromagnetics and microwave, ultra wide band antenna, multi input multi output antenna and diversity antenna.